CHAPTER 2

LITERATURE REVIEW AND OBJECTIVES

2.1 Literature review

In this chapter, a thorough literature review is reported on fundamentals of microfluidic fuel cell (MFC), various types of MFC, fabrication techniques, major component, characterization of electrodes and MFC performance using glycerol fuel. Finally, major research gaps are identified based on the exhaustive literature review on glycerol based microfluidic fuel cell for further development to generate low cost electricity. After identifying the major research gaps, the objectives of the thesis are decided which are presented at the end of this chapter.

2.1.1 Fundamentals of microfluidic fuel cell

The membraneless microfluidic fuel cell is also known as laminar flow fuel cell (LFFC) which follows similar electrochemical principles as that of membrane electrolyte based conventional fuel cell. The ion transport in conventional fuel cell occurs through the membrane electrolyte like Nafion$^®$ or liquid electrolyte KOH, H_2SO_4 etc. A large distance in the range of micrometre to millimetre is maintained between two electrodes using membrane electrolyte or liquid electrolyte. Whereas, in microfluidic fuel, the laminar nature of flow with low Reynolds number (Tanveer and Kim 2017) maintains separation between fuel and oxidant stream, whose interface acts as virtual membrane for ion transport. The streams in microfluidic fuel cell containing the fuel and oxidant, which are allowed to flow side by side through a single microfluidic channel of width < 1 mm (Kjeang et al., 2009). The MFC device eliminates the issues related to polymer electrolyte membrane based fuel cells like fuel crossover, membrane degradation and dehydration at

high temperature. On the other side, these co-laminar configurations in microfluidic fuel cell also allow selection of electrolyte independently at anode and cathode streams e.g., mixed media type (Kjeang et al., 2009). Thus, it provides an opportunity to enhance the reaction rates and cell voltage both. Moreover, miniaturization of fuel cells has advantage of high surface to volume ratio and it is well known that electrochemical reactions are surface based and thus, the fuel cell efficiency is enhanced. The most prominent advantage related to microfluidic fuel cell is the economical aspect. Microfluidic fuel cells can be manufactured by inexpensive, well established micromachining and microfabrication methods and the cost associated with the membrane, which is significant for most of the conventional fuel cells, is eliminated. Moreover, microfluidic fuel cells are normally operated at room temperature and require no humidification, water management, or cooling systems (Kjeang, 2014).

The laminar flow is established in the fluid streams within the microchannel at low Reynolds number. At low Reynolds number, the surface tension or viscous effect i.e., surface effects lead over the inertia effects which is volume based effect. This contributes to achieve co-laminar flow with restricted liquid-liquid interface in a microchannel. The continuum and laminar flow nature of liquid in the microchannels and conservation of mass of the fluid in the microchannel stream follows the continuity equation due to its laminar flow nature in microchannels as shown in Equation (2.1). Where, ρ is the density and $\vec{u}$ is the velocity field.

$$\frac{\partial \rho}{\partial t} + \nabla(\rho \vec{u}) = 0 \qquad\qquad (2.1)$$

At constant density flow, the Equation (2.1) is reduced to $\vec{u} = 0$. The velocity field is calculated using Navier-stokes equation (Equation (2.2)).

$$\rho \left(\frac{\partial \vec{u}}{\partial t} + \vec{u} \nabla \vec{u} \right) = -\nabla p + \mu \nabla^2 \vec{u} + \vec{f} \qquad\qquad (2.2)$$

Where, p is pressure, μ is viscosity and f summarizes the body forces per unit volume. The pressure drop, ∇p for laminar flow in the microchannel can be calculated by finding the hydraulic diameter D_h, length of the microchannel L and average velocity V is the given formula by Equation (2.3). Whereas, the pumping power for anode and cathode streams is calculated by the product of pressure drop and flow rate Q as shown in Equation (2.4) (Kjeang et al., 2009).

$$\nabla p = \frac{32\mu L V}{D_h^2} \qquad\qquad (2.3)$$

$$W = \frac{32\mu L V Q}{D_h^2} \qquad\qquad (2.4)$$

The assumption considered for calculating the pumping power derived from Equation (2.4) is that the flow is fully developed in the microchannel, and minor losses due to the inlet and outlet stream are ignored (Kjeang et al., 2009).

Peclet number and Schmidt number is also important dimensionless number to avoid the intermixing of liquid-liquid interface. In microfluidic fuel cell devices, very high Peclet number, $Pe = \frac{V D_h}{D}$ are observed i.e., the transverse diffusion rate is smaller than the convective velocity, thus the diffusive mixing is limited to a thin interfacial width in the centre of the channel that grows as a function of downstream position (z) and average velocity (V) (Kjeang 2014). Moreover, Schmidt number, $Sc = \frac{\mu}{\rho D}$ which is the ratio of momentum diffusivity and mass diffusivity, for the high value indicates that the viscous effects is more than concentration effects revealing the concentration boundary layer to a linear velocity profile (Choban et al., 2004). Where, μ is kinematic viscosity, ρ is the

density of liquid, D is diffusivity of the species in the solvent and D_h is the hydraulic diameter.

The crossover effect and inter diffusion width can also be reduced by adjusting the flow rates of anode and cathode streams. The inter diffusion zone generated from the flow of two streams which has an hourglass shape with maximum width (δ_x) or broadening at the channel walls according to the following Equation (2.5).

$$\delta_x \propto \left(\frac{DHz}{V}\right)^{1/3} \tag{2.5}$$

Where, H is the channel height, z is the downstream distance, V is the average velocity and D is the diffusion coefficient of species under consideration.

The ohmic resistance, R_f due to the ionic transport in the microchannel determined by the charge transfer distance (d_{ct}) occurred due to electrode gap, the cross-sectional area for charge transfer (A_{ct}), and the ionic conductivity (σ), is given by Equation (2.6):

$$R_f = \frac{d_{ct}}{\sigma A_{ct}} \tag{2.6}$$

The fuel and oxidant streams enter the channel and then reacted at anode and cathode, respectively to generate electrical current. The current density distribution is predicted by Butler-Volmer equation as shown in Equation (2.7) (Carrette et al., 2001):

$$j = j_0 \left[\exp\left(\frac{\alpha_a F\eta}{RT}\right) - \exp\left(\frac{\alpha_c F\eta}{RT}\right)\right] \tag{2.7}$$

Where, the anodic and cathodic charge transfer coefficients are represented by α_a and α_b, respectively. T, R, F and η represents the operating temperature, universal gas constant, Faraday's constant and surface overpotential, respectively.

The fuel utilization is defined as the ratio of fuel electrochemical consumed by the cell and the fuel actually supplied to the fuel cell. However, at slow flow rate the depletion zone over the electrode surface increase. Thus, the increase in flow rate of fuel replenished the depletion zone over the electrodes and gives the maximum cell performance with low fuel utilization (Shaegh et al., 2011). The fuel utilization can be calculated by the given Equation (2.8):

$$\varepsilon_{fuel} = \frac{J}{nFV_{fuel}}$$
(2.8)

In the given formula (Equation (2.8)), the produced cell current density is denoted by J, number of moles of electron transferred is denoted by n, Faraday constant is denoted by F, and V_{fuel} represents fuel input rate in mol/sec. In the next section, various types of the microfluidic fuel cell devices are discussed.

2.1.2 Types of microfluidic fuel cell

Generally, the conventional fuel cells are classified based on the electrolyte used such as proton exchange polymer electrolyte membrane fuel cell (PEMFC), alkaline fuel cell (AFC), phosphoric acid fuel cell (PAFC), molten carbonate fuel cell (MCFC) and solid-oxide fuel cells (SOFC). Direct ethanol fuel cell (DEFC) and direct methanol fuel cell (DMFC) are named based on fuel used. However, the microfluidic fuel cell is classified by its geometry such as Y-shaped, T-shaped, I-shaped and F-shaped (Kjeang et al., 2009). Due to recent advanced research development activities on microfluidic fuel cells, they are also categorized based on the fluid delivery in microchannel i.e., fuel and oxidant and their phase of transport irrespective of the cell geometry and architecture. The classification of MFC based on reactant phase are (i) liquid fuel and liquid oxidant type and (ii) liquid fuel and gaseous oxidant type.

For the type of "liquid fuel and liquid oxidant", fuel and oxidant is supplied in liquid state. The liquid fuels are mainly alcohols methanol (Rathoure and Pramanik 2016), ethanol (Armenta et al., 2016) and glycerol (Maya-Cornejo et al., 2016), others are formic acid (Zuria et al., 2014) and glucose (Galindo et al., 2014) etc. The liquid oxidants used in MFCs are hydrogen peroxide (Rathoure and Pramanik 2016) and potassium permanganate (Choban et al., 2004). This type of liquid fuel and liquid oxidant has an important advantage of wide range of pH variation as there is no membrane electrolyte. This combination also allows testing of various type of supporting electrolyte in the MFC. The other type "liquid fuel and gaseous oxidant" is low cost, as it uses easily available gaseous oxidant i.e., atmospheric oxygen in MFCs. It is reported in literature that the oxygen reduction at cathode side is a slow kinetics reaction which affects MFCs performance. Thus, to increase the reaction kinetics at cathode, atmospheric oxygen from air was used in many studies. Moreover, the oxygen as oxidant can be introduced by dissolving it in the KOH electrolyte (Dector et al., 2013a). Jayashree et al., (2005) first reported the exclusion of the use of dissolved oxygen by introducing the idea of an air breathing cathode concept that improved the performance of this cathode side reaction tremendously (Figure 2.1).

Moreover, the diffusion coefficient of oxygen from atmosphere is four times higher in magnitude in air than in an aqueous solution. Rathoure and Pramanik (2016) also adopted the same combination for the electrooxidation of ethanol in air breathing MFC. There are many researchers are working on air breathing microfluidic fuel to enhance the cathode mass transfer rate and to improve the cell performance (Zou et al., 2016; Zhou et al., 2020). Thus, in the present study, Y-shaped and T-shaped air breathing MFC is used with liquid fuel and gaseous oxidant based on reactant phases.
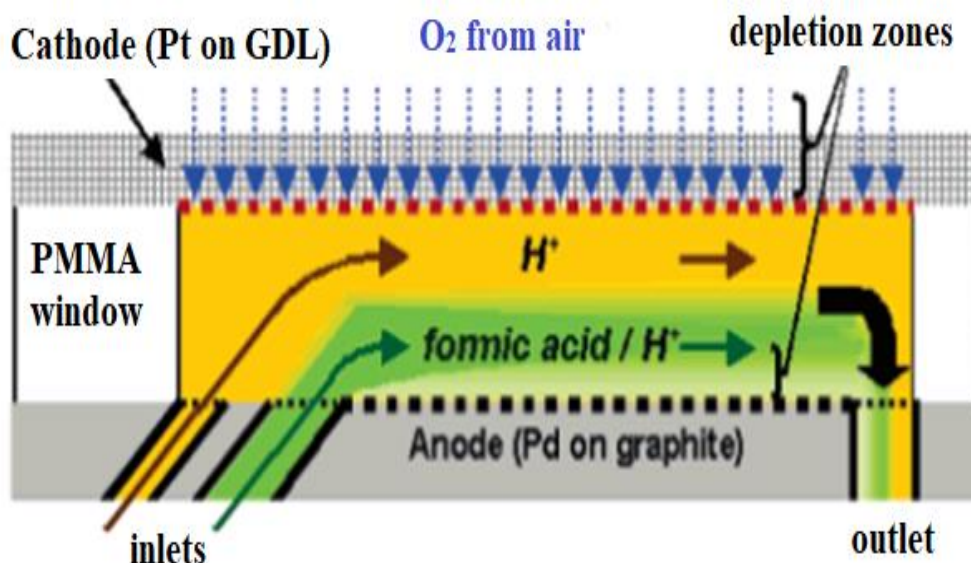
Figure 2.1 An F-shaped air breathing microfluidic fuel cell captures oxygen from the surrounding air via gas diffusion through the 'dry' side of the porous cathode structure (Jayashree et al., 2005).

2.1.3 Microfluidic fuel cell fabrication techniques

Sophisticated micromachining techniques are generally used to fabricate microfluidic fuel cell devices. As already discussed, the microfluidic fuel cell device comprised of a microchannel, where two electrodes are fitted to maintain the gap between two electrodes less than 1 mm and thereby maintaining laminar flow of anode and cathode streams. The key criteria for choosing micromachining technique are the structural material, microstructure scale and structure complexity. In most of the fabrication of MFC, the materials used are poly methyl methacrylate (PMMA) polymer sheets and polydimethylsiloxane (PDMS) (Kjeang et al., 2007; Feali et al., 2014). The microchannel in the sheets can be fabricated using Xerography, micromolding, hot embossing, and micromilling (Diaz-Real et al., 2016). Moreover, laser assisted techniques such as photolithography, laser ablation and stereo lithography are also used for MFC fabrication. The micromilling is a simple procedure where computer numerical control (CNC) micromilling cutters are used. This technique is suitable for rigid PMMA sheets

(Rathoure and Pramanik 2016). Xurography is an economically feasible and quick process technique (Renaud et al., 2015). It uses a plotter cutter where the channels are drawn in a shielding mask placed over the substrate and a conductive layer is then placed over the substrate. The mask is finally taken out leaving the conductive layer printed on the substrate. This technique is exclusively used for the fabrication of microchannels and electrodes (Renaud et al., 2015). Similar type of techniques is used in micromolding and hot embossing. In micromolding technique, a liquid resin is placed in a mould with the desired shape in micromolding and dried by heat at room temperature. In hot embossing techniques, a solid polymer is heated to soften the material in hot embossing, and then thermoformed by heat and pressure. Fabrication technique for microchannel in MFC is very crucial step. The machines or equipment for fabrication is showed be easily available and accessible, simple technique, less time taking and inexpensive.

The first microfluidic fuel cell was developed by Ferrigno et al., (2002) using PDMS material and soft lithography technique to fabricate a microchannel with two inlets and one outlet having thickness of the microchannels of 200 µm. The microchannel for narrow channels (h ≈ 50 µm) can also be fabricated by SU-8 photoresist using lithography technique. Kjeang et al., (2007) fabricated Y-shaped microfluidic fuel cell for vanadium redox species using poly dimethylsiloxane (PDMS) for top layer and polyurethane for base layer and fitted in a customized aluminium holder with grooves that isolates the bands by 1.2 mm and grip them in place. The top layer of the Y-shaped microfluidic fuel cell with a dimension of 2 mm wide and 120 µm height was made in PDMS by replica moulding. Feali et al., (2014) used PMMA for fabrication of microfluidic fuel cell with finny electrodes and the metal material was used to make the electrodes. Arjona et al., (2015) fabricated an air breathing microfluidic fuel cell containing two PMMA plates, the cathode was made of carbon paper and an SU-8 pattern covered with Vulcan[®] carbon as

anode. The microchannel for fluid flow was made of PDMS material. The window for air breathing was kept in the PMMA plate close to the cathode with active area of 0.9 cm^2 of electrodes. The cold spray technique was used for electrocatalysts deposition on the electrodes surface.

Recently, Rathoure and Pramanik (2016) fabricated T-shaped air breathing microfluidic fuel cell using PMMA sheet with the help of CNC milling cutter. Desmaële et al., (2016) fabricated microfluidic fuel cell for the study of ethanol electrooxidation in enzymes immobilized onto cantilevered porous electrodes, the entire structure was guided by CNC machine. The CNC milling machine is also used for the microchannel fabrication in conventional fuel cell (Jang and Park 2010; Scotti, 2014).

Among all these fabrication techniques micromilling using a CNC cutter is common for its simplicity and quick fabrication method. Generally, MFC channels are made by CNC cutter in standard machine shop equipment. The computer numerical control (CNC) technique is quick and appropriate method for fabrication of microchannels (Kjeang et al., 2007). The CNC machine can be used to design the microchannel for microfluidic fuel cell devices in a PMMA sheet in a very simple way and thus used for air breathing MFC fabrication in the present study.

2.1.4 Components of microfluidic fuel cell

The microfluidic fuel cell consists of anode and cathode electrodes, electrolyte, fuel and oxidant. The active component of anode and cathode is electrocatalyst. Electrolyte for MFCs are liquid in nature which are generally fed to the microchannel mixed with anode fuel and cathode oxidant. The electrocatalysts material, fuel, oxidant and electrolyte are discussed in the subsequent sections.

2.4.1.1 Electrode materials

The electrodes are essential part of the microfluidic fuel cell devices, where anodic and cathodic reaction take place to generate current. The active material used to fabricate electrode is electrocatalyst which is mixed with Nafion$^®$ ionomer, Polytetrafluoroethylene (PTFE) dispersion, activated carbon isopropanol to prepare electrocatalysts ink. The ink is deposited on a substrate called gas diffusion layer (GDL). Toray carbon paper or carbon cloths are generally used as GDL for electrode preparation. As already mentioned, the MFC performance depends upon the selection of electrocatalyst based on fuel, oxidant and electrolyte medium i.e., acidic or alkaline. The most active component of an electrode is the electrocatalyst which actively take part in the electrooxidation at anode and reduction processes at cathode of the cell. There are different types of electrocatalysts so far are used for anode and cathode fabrication of a glycerol based MFC.

2.1.4.1.1 Anode electrocatalyst for glycerol electrooxidation

The electrochemical conversion of alcohol is a complex multistep process which comprises the adsorption of alcohol, breaking of inter-atomic bond, transfer of charge, reactions between the species and product desorption (Zhang et al., 2014, Baranton and Coutanceau 2013; Guerrero-Pérez et al., 2009; Gomes and Tremiliosi-Filho 2011). Thus, the effectiveness of anode reaction dependents upon (i) the interaction between the electrocatalyst surface and alcohol molecules, (ii) the interaction between absorbed species and electrocatalyst surface, and (iii) oxide formation. The reaction mechanism for glycerol electrooxidation depends upon many factors like electronic properties of electrocatalyst and type of electrolyte medium i.e., acidic or alkaline (Simoes et al., 2010, Gomes and Tremiliosi-Filho 2011). Thus, the selection of electrocatalyst for glycerol electrooxidation reactions is important due to the complex structure of glycerol where three carbon atoms are attached with three OH groups which is already mentioned in the

introduction (page no. 9). The C-C bonds of the complex structure are difficult to break down through the electrooxidation process using present electrocatalyst. The platinum (Pt) and palladium (Pd) based electrocatalyst Pt/C and Pd/C have been used widely for the glycerol electrooxidation reaction studies, due to their high activity and excellent stability in both acidic and alkaline medium. The performance of Pd/C for glycerol electrooxidation in alkaline medium is comparable to Pt/C electrocatalyst and plausible substitutes for Pt based electrocatalysts since Pd is less expensive and available 50 times more abundant on earth than Pt (Alaba et al., 2020). Several research works have been carried out using single metal Pd and Pt electrocatalyst for glycerol electrooxidation (Wang et al., 2014; Nascimento and linares 2014; Martins et al., 2018a; Martins et al., 2019; Zhang et al., 2012). Recently, many studies have also been carried out on glycerol electrooxidation using Pt and Pd based bimetallic electrocatalyst like Pt-Pd (Rezaei et al., 2016, Bhunia et al., 2018), Pt-Au (Ottoni et al., 2016; Li et al., 2017), Pt-Ru (Da Silva et al., 2017; Zhou et al., 2018; Do valle et al., 2015), Pt-Ag (Garcia et al., 2017; Kim et al., 2014), Pt-Bi (Gonzalez-Cobos et al., 2016), Pt-Cu (Rezaei et al., 2016; Zhai et al., 2018), Pt-Co (Zhai et al., 2018), Pt-Sn (Da Silva et al., 2017; Do valle et al., 2015, Prasanna and Selvaraj 2015), Pd-Sn (Zalineeva et al., 2015) and Pt-Ni (Da Silva et al., 2017; Zhou et al., 2018), Pd-Au/C (Simoes et al., 2010; Mougenot et al., 2011), Pd-Ni/C (Simoes et al., 2010, Lee et al., 2012; Holade et al., 2013), Pd-Pt-Bi/C (Simoes et al., 2011) and Pd/TiO$_2$ nanofibres (Su et al., 2009). However, the Palladium based electrocatalysts show excellent results for glycerol electrooxidation. It should be noted that the electrocatalysts for glycerol electrooxidation are not available commercially in the market. Most the bimetallic electrocatalysts have been synthesized in laboratory and further characterized in the half cell (Holade et al., 2013; Zalineeva et al., 2015) or in the single cell microfluidic fuel cell (Maya-Cornejo et al., 2016) for glycerol electrooxidation.

Thus, a scope is still there to develop a suitable and low cost bimetallic electrocatalyst for efficient power generation from the glycerol based MFC using atmospheric oxygen as oxidant. Moreover, thorough literature review shows that Pd-Pt/C and Pd-Ni/C electrocatalyst of suitable composition have not been studied and their detailed performance study in glycerol based MFC are not found in open literature. Thus, in the present thesis work, synthesis of bimetallic Pd-Pt/C and Pd-Ni/C electrocatalyst of various metal ratios were considered for anode of MFC. The selection of cathode electrocatalyst is also important as shown that of anode to achieve better MFC performance. The cathode electrocatalyst are discussed in the next section.

2.1.4.1.2 Cathode electrocatalyst

In all types of fuel cells, the cathodic reaction of oxygen reduction plays an important role for the generation of current and is also considered as the main limiting factor which control the performance of the fuel cell (Basu, 2007; Wang et al., 2005). The fuel cells directly generate electricity by electrochemically oxidizing fuel and reducing oxygen to produce water as the only byproduct in case of hydrogen oxygen fuel cell. However, using alcohols as a fuel the end product is mainly H_2O and CO_2 (Ong et al., 2017).

The Pt supported on carbon (Pt/C) electrocatalyst is usually used as electrocatalyst for the ORR at the cathode (Lee et al., 2015). In microfluidic fuel cell devices, commercial Pt/C is mainly used as cathode electrocatalyst (Cohen et al., 2005; Mitrovski et al., 2004, Jayashree et al., 2005; Hasegawa et al., 2005; Salloum et al., 2008, Rathoure and Pramanik 2016; Pramanik and Rathoure 2017). However, many researchers have significantly worked to develop Pt-alloyed electrocatalysts to enhance the electrocatalytic activity and stability to reduce the consumption of costly Pt electrocatalyst. Zhang et al., (2007) studied on the Pt electrocatalyst surface alloyed with Au to improve the stability for ORR. Lim et al., (2009) synthesized Pd−Pt alloy electrocatalyst having high activity

for ORR. The transition metal Ni alloyed with Pt also significantly improved the oxygen reduction as reported by Stamenkovic et al., (2002); Stamenkovic et al., (2007) and Chen et al., (2014). Pt-Cu (Mani et al., 2008; Gupta et al., 2009) alloy also shows improved electrocatlytic activity and stability.

Although Pt based bimetallic electrocatalyst are tested for oxygen reduction, Pt/C is the widely used cathode electrocatalyst for oxygen reduction for faster reaction in alkaline medium (Ramaswamy and Mukerjee 2012). Thus, in the present research work, commercial Pt/C was selected as cathode electrocatalyst. As the laboratory synthesized electrocatalyst is used at anode of MFC and thus, the electrocatalyst preparation technique for anode electrocatalyst is discussed in the following section.

2.1.4.1.3 Anode electrocatalyst preparation techniques

There are several techniques so far reported in the literature for synthesis of electrocatalyst used for glycerol electrooxidation in half cell and MFC cell studies. The various synthesis routes produce electrocatalyst of varying properties which are surface morphology, particle size crystallite size and surface area. All these properties control the electrochemical activity of the synthesized electrocatalysts. The frequently used important methods for electrocatalyst synthesis are sol-gel, co-precipitation, impregnation reduction method, colloidal method and microemulsion method. The synthesized electrocatalyst are reduced either by in-situ method like polyol reduction method (Choudhary and Pramanik 2019), $NaBH_4$ reducing agent (Sudirman et al., 2020), formic acid (Antolini et al., 2007) or after synthesis of electrocatalysts by hydrogen reduction method (Panjiara and Pramanik 2020a). Among all these methods, impregnation reduction method is very popular due to its several advantages like very fast method, cheaper, simple, efficient and scalable to synthesized electrocatalysts (Zhu et al., 2015). Thus, impregnation reduction method was selected for synthesis of Pd based single and bimetallic electrocatalyst in the

present study. Zhang et al., (2012) synthesized Au/C electrocatalyst through a modified solution phase-based nanocapsule method for anion exchange membrane based direct glycerol fuel cell. In this method, the required quanity of precursor $AuCl_3$ was first dissolved in a mixture of octadecene and oleylamine under nitrogen flow environment. Further, the solution was quickly heated to 80 ^{o}C, afterwards lithium tri ethyl borohydride was quick injected. The temperature was maintained for 10 min then the solution was cooled down to room temperature and then separated by centrifugation. Finally, the Au-NPs were deposited on Vulcan® XC72R carbon black to make a desired percentage of Au/C electrocatalyst. Dector et al., (2013a) synthesized Pd/C and Pd/MWCNT using impregnation synthesis method and reduced using $NaBH_4$. In this process, at first the carbon black and MWCNTs were dispersed in deionized water in ultrasonic bath for 60 min. Further, the dispersed carbon black and MWCNTs were added into the precursor $(NH_4)_2PdCl_6$ aqueous solution. The reduction process was performed by adding $NaBH_4$ slowly into this solution and vigorously stirred for 1h. Finally, the resulting solution was filtered, washed and dried overnight at 60 ^{o}C to get the desired electrocatalyst. Ottoni et al., (2016) synthesized Pd (20 %)/C, Au (20 %)/C, and PdAu (20 %)/C for glycerol electrooxidation using the sodium borohydride reduction method. The procedure starts with the dilution of metal precursors by adding water/2-propanol (50/50, v/v) mixture. Further, the carbon Vulcan® XC72R support material was dispersed in the solution and kept in ultrasonic bath for 10 min. The reduction process was performed by adding excess $NaBH_4$ and 0.1 mol/l NaOH and kept for 30 min under stirring at room temperature. Finally, the mixture was filtered and the resultant catalyst was washed with 2 L of distilled water and dried at 70 °C for 2 h to get the desire product. Geraldes et al., (2015) synthesized a series of Pd based bimetallic and trimetallic electrocatalyst using an electron beam irradiation reduction method for alkaline direct glycerol fuel cell. At, first

the desired amounts of metal precursors were dissolved in 50/50 (v/v) water/2-propanol. The carbon Vulcan® XC72R support material was then, introduces into the solution using an ultrasonic bath. Then the obtained mixture at normal condition was continuously stirred under electron beam irradiation. Finally, the mixtures after electron beam irradiation were filtered and the solids were washed with water and dried at 70 C for 2 h to obtain the desired electrocatalyst. Holade et al., (2013) used a new method called "bromide anion exchange" to synthesize different compositions of PdNi/C and PdAg/C with 30 wt% metal loading for electrooxidation of glycerol in alkaline medium. This new method is free from surfactant. At first the metal precursors is taken based on the different atomic ratios and then dissolved in ultrapure water, and KBr was introduced as an anion exchange agent. The bromide ion substitutes the chloride which gives a significant steric environment. The colour of the Pd salt aqueous solution changes from yellow to brown after the addition of KBr results in the formation of the $[PdBr_4]^{2-}$ complex. Furthermore, required amount of pre-treated under N_2 atmosphere at 400 °C for 4 h carbon (Vulcan® XC72R) was added. In the next step, the mixture was kept for ultrasonication for 45 min to achieve a good dispersion. It was reduced by pouring 0.1 mol/l $NaBH_4$ reducing agent into the mixture and continuously stirred at 40 °C for 2 h. In the last step, the mixture was filtered and washed several times with ultrapure water to remove all ionic species and the residue was dried in an oven at 40 °C for 12 h to achieve the desire electrocatalyst. Li et al., (2017) investigated Pt/C and Pd/C catalysts promoted by Au for glycerol electrooxidation in alkaline medium using reduction method. The PtAu/C electrocatalysts on the support material carbon black were synthesized by reduction of the precursors. The Pt precursor was H_2PtCl_6 and Au was $HAuCl_4$, respectively. The solution was prepared in distilled deionized water solution and reduced using an excess 0.01 mol/l $NaBH_4$ solution. Similarly, the PdAu/C catalysts were prepared by reduction of Pd precursor $Pd(NH_3)_4Cl_2$

Au precursor and HAuCl$_4$ solution. Zalineeva et al., (2015) prepared Pd$_1$Sn$_x$ catalysts with different Pd/Sn atomic ratios were synthesized using the sacrificial support method (SSM) for glycerol electrooxidation in alkaline medium. At first, known amount of silica was dispersed in water using ultrasonication technique. Then, the desired amounts of metal precursors were added into the silica suspension and the mixture was kept overnight for drying. The dried material was reduced under hydrogen at 300 ^{o}C for 2h. After the reduction process, the silica template was detached by etching in 7M KOH solution and then continually washing with distilled water until neutral pH was achieved. From the thorough literature review, it is seen that the most commonly used method for electrocatalyst preparation is impregnation reduction method (Bock et al., 2008; Dector et al., 2013a) which diminishes the filtration and washing processes in the electrocatalyst preparation techniques. Impregnation reduction method process is quicker, cheaper and allows the final property and configuration to be monitored in advance (Deraz, 2018). Thus, impregnation reduction method was selected for electrocatalyst preparation in the present study. The various techniques used for electrochemical and physical characterization of synthesized electrocatalyst are discussed in the next section.

2.1.4.1.4 Electrochemical characterization

2.1.4.1.4.1 Electrochemical characterization of anode electrocatalysts

The cyclic voltammetry (CV) is an effective electrochemical technique for studying electrode reactions (Bard and Faulkner 2002). The CV technique is very important and frequenty used because they provide an important experimental knowledge and insights into the kinetic and thermodynamic details of many electrochemical systems (Sandford et al., 2019). For a given electrochemical system, the peak characteristics in a cyclic voltammogram may be used to gain qualitative information on the relative rates of reaction and reactant diffusion. When the potential of the working electrode is more

positive than that of a redox couple, the corresponding reactants may be oxidized and produce an anodic current. Due to intrinsic reaction mechanisms, a cyclic voltmogram may have several cathodic and anodic peaks (Elgrishi et al., 2018). Thus, the presence of the reactive intermediate and the inactive intermediates i.e., poisoning species produced from the glycerol electrooxidation in an alkaline solution could be investigated. The electrooxidation of glycerol is a complex reaction and form several intermediate products (Simoes et al., 2010). Generally, the electrooxidation of glycerol on Pt and Pd electrocatalyst, the primary OH group oxidized easily with the formation of glyceraldehyde, glyceric acid and tartronic acid. Whereas, the second OH group are difficult to oxidized at low potentials and gives dihydroxyacetone, hydroxypyruvic acid and mesoxalic acid which are observed only at high potential range. Moreover, the formation of glycolic acid, oxalic acid and formic acid are also identified which indicates the breaking of the C–C bond (Roquet et al., 1994; Simoes et al., 2010). Kwon et al., (2010) proposed the reaction mechanism of glycerol electrooxidation in alkaline medium using Pt and Au electrodes (Figure 2.2).
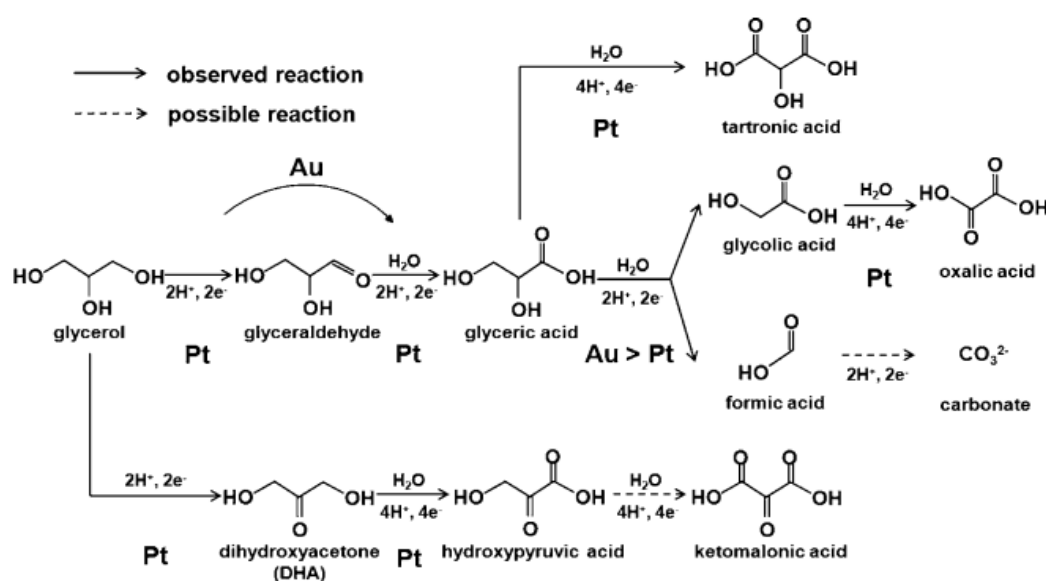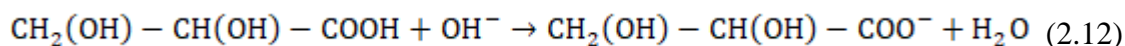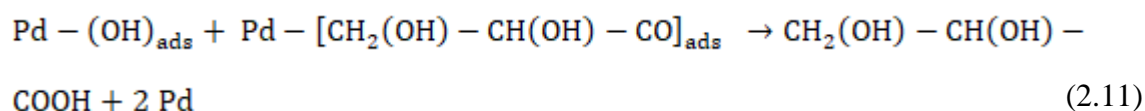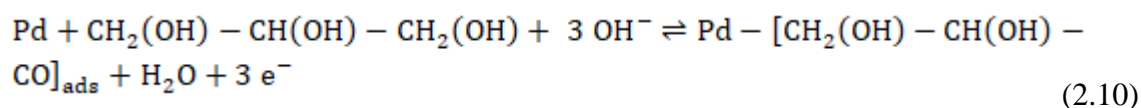

Figure 2.2 Glycerol electrooxidation mechanisms on Au and Pt electrodes in alkaline media.

The glycerol fuel is first oxidized during a two electron transfer stage to glyceraldehyde in the process of primary alcohol oxidation, which is further oxidized to glyceric acid in the next stage of two electron transfer process. Glyceric acid is further oxidized as a next two electron transfer step by cleavage of a C-C bond into glycolic acid and formic acid on both Pt and Au electrodes. Moreover, glyceric acid and glycolic acid are then oxidized to form tartronic acid and oxalic acid on the platinum electrode, respectively. Dihydroxyacetone is formed by a two electron transfer step, but only on the Pt electrode in the process of secondary alcohol oxidation. Dihydroxyacetone is oxidized to hydroxypyruvic acid as a next two electron transfer step, which can be further oxidized to ketomalonic acid, although it has not been detected, due to system detection limit. The formation of CO_2 as the final oxidation product of glycerol on a gold electrode was observed recently in alkaline media during FTIR experiments, although CO_2 should appear as carbonate (CO_3^{2-}) in alkaline media through its combination with OH.

Another proposed reaction mechanism of glycerol electrooxidation pathway on Pd in alkaline medium is presented below (Equation 2.9 to Equation 2.12) (Kahyaoglu et al., 1984; Su et al., 2009).

$$Pd + OH^- \rightleftharpoons Pd - (OH)_{ads} + e^- \tag{2.9}$$

$$Pd + CH_2(OH) - CH(OH) - CH_2(OH) + 3\,OH^- \rightleftharpoons Pd - [CH_2(OH) - CH(OH) - CO]_{ads} + H_2O + 3\,e^- \tag{2.10}$$

$$Pd - (OH)_{ads} + Pd - [CH_2(OH) - CH(OH) - CO]_{ads} \rightarrow CH_2(OH) - CH(OH) - COOH + 2\,Pd \tag{2.11}$$

$$CH_2(OH) - CH(OH) - COOH + OH^- \rightarrow CH_2(OH) - CH(OH) - COO^- + H_2O \tag{2.12}$$

This pathway shows that the kinetic effects of the electrooxidation of glycerol are improved by increasing OH^- levels, which generate more OH^- exposure on the Pd surface (Equation (2.9 to 2.12). Furthermore, the adsorption of glycerol in the Pd active sites was promoted by the Equation (2.2) in the presence of higher amount of OH^- ions. This causes a higher peak current and negative shift of peak potential. However, the more adsorption of OH^- in more alkaline electrolytes ($C_{OH-} > 3$ M) prevents glycerol adsorption at the Pd sites and thus reduces the reaction rate of glycerol oxidation. Thus, from the above discussed reaction pathway it is seen that Pd electrocatalyst is more active for glycerol electrooxidation in alkaline medium due to improved kinetic effects of the electrooxidation of glycerol by increased OH^- levels on the Pd surface.

There are many such studies have been reported on various types of synthesized electrocatalysts to evaluate their activity. The details of the electrochemical process used and outcomes for the glycerol electrooxidation using various synthesized electrocatalyst are presented in Table 2.1.

Table 2.1 Performance comparison of different electrocatalyst for glycerol electrooxidation in half cell study.

References	Anode electrocatalyst/ Electrolyte used	Electrocatalyst preparation method/ Electrode material or substrate	Electrochemical techniques/Investigation purpose	Remarks
Mougenot et al.,(2011)	Electrocatalyst: PdAu Electrolyte: NaOH	Plasma sputtering method; Glass carbon electrode	Cylic voltammetry; Study of glycerol electrooxidation	Plasma sputtering method shows more active bimetallic PdAu material than wet chemistry method, due to improved electrode structure and surface composition. The glycerol adsorption on palladium surface and hydroxyl species formation on gold surface increases the catalytic activity enhancement through the bifunctional mechanism.
Lee et al., (2012)	Electrocatalyst: $Pd_3Ni_1/C, Pd_2Ni_1/C, Pd_1Ni_1/C$ Electrolyte: H_2SO_4	Colloidal method; Glassy carbon disk electrode	Cyclic voltammetry, Chronoamperometry; Study of glycerol electrooxidation	Addition of Ni to a Pt catalyst significantly improves the electrocatalytic activities for glycerol electrooxidation. Chronoamperometry tests shows that Pt_2Ni_1/C catalysts have the highest current density and lowest decay rate for current density compared with the Pt/C.

References	Anode electrocatalyst/ Electrolyte used	Electrocatalyst preparation method/ Electrode material or substrate	Electrochemical techniques/Investigation purpose	Remarks
Habibi et al., (2012)	Electrocatalyst: Au, Pd and Pt Nano particles Electrolyte: NaOH	Sol-gel processing method ; Carbon ceramic electrode	Cylic voltammetry, Chronoamperometry, chronopotentiometry and electrochemical impedance spectroscopy; Study of glycerol electrooxidation	Cylic voltammetry indicated that the Pt/CC has the lowest onset potential. Chronoamperometry and chronopotentiometry studies showed that the Au/CC has significant electrocatalytic activity for glycerol oxidation. Pd/CC showed a higher kinetics compared to two other electrodes for glycerol oxidation. EIS showed that Pd/CCE has better poisoning tolerance compared to two other electrodes.
Oliveira et al., (2014)	Electrocatalyst: FeCoNi/C, CoNi/C, FeNi/C,Ni/C Electrolyte:NaOHNaOH	Impregnation method; Toray carbon paper electrode	Cylic voltammetry In situ FTIR, HPLC; Study of glycerol electrooxidation	The Ni-based electrocatalyst i.e., Ni/C and FeCoNi/C exhibited best conversion of glycerol to formate and glycolate, and CoNi/C showed the highest glycerol conversion.

References	Anode electrocatalyst/ Electrolyte used	Electrocatalyst preparation method/ Electrode material or substrate	Electrochemical techniques/Investigation purpose	Remarks
Holade et al., (2013)	Electrocatalyst: PdNi/C, PdAu/C in different ratios, Electrolyte: NaOH	Bromide anion exchange method; Glassy carbon	Cyclic voltammetry, IR spectroscopy; Study of glycerol electrooxidation	Ni and Au elements in the bimetallic electrocatalyst modify the electronic properties of Pd to shift the onset potential at lower values for CO and glycerol oxidation. This electrochemical behavior shows more active sites of materials are localized on the planes with high coordination numbers.
Zalineeva et al., (2015)	Electrocatalyst: PdSn, $PdSn_2$, $PdSn_3$ Electrolyte: KOH	Sacrificial support method; Glassy carbon disk	Cyclic voltammetry In situ FTIR; Study of glycerol electrooxidation	The modification made by Sn on Pd decreases the onset potential for glycerol electrooxidation from 0.6 V for pure Pd down to 0.45 V for Pd_1Sn_1. Presence of Sn eliminates the capability of Pd to activate the dissociative adsorption of glycerol with C-C bond breaking and suppress the formation of CO_3^{2-} and CO_2.

References	Anode electrocatalyst/ Electrolyte used	Electrocatalyst preparation method/ Electrode material or substrate	Electrochemical techniques/Investigation purpose	Remarks
Li et al., (2017)	Electrocatalyst: Pt/C and Pd/C catalysts promoted by Au; Electrolyte: KOH	Reduction method; Graphite rod	Cyclic voltammetry; Study of glycerol electrooxidation	Addition of Au can promote the catalytic activity and stability of Pt/C and Pd/C for glycerol electrooxidation. Weight ratio of 4:1 for Pt to Au and Pd to Au gives best performance for electrooxidation of glycerol. More negative onset potential is attained with adding Au.
Sandrini et al., (2018)	Electrocatalyst: Pt (111) Electrolyte: NaOH	Method: Not available Pt (111) electrode	Cylic voltammetry, In situ FTIR; Study of glycerol electrooxidation	Pt (111) electrode suffers strong deactivation once the surface attains potentials higher than 0.8 V. In situ FTIR shows carboxylates and acyl are the key intermediates formed during the GEOR.

2.1.4.1.4.2 Electrochemical characterization of cathode

The oxygen reduction reaction (ORR) has two primary pathways i.e., single step 4 e^- pathway and the other is two step $(2+2)$ electron (e^-) pathway in alkaline medium presented below (Rathoure and Pramanik 2016) (Equation (2.13) to (2.15)):

$$O_2 + H_2O + 4e^- \rightarrow 4OH^- \tag{2.13}$$

or,

$$O_2 + H_2O + 2e^- \rightarrow HO_2^- + OH^- \tag{2.14}$$

$$HO_2^- + H_2O + 2e^- \rightarrow 3OH^- \tag{2.15}$$

The ORR mechanism on Pt normally proceeds through a 4 electrons progression due to (i) shortening of Pt-Pt interatomic distance favourable for the dissociative adsorption of O_2 (geometric effect), (ii) increased d-band vacancies creating a strong metal O_2 interaction and then weakening the O–O bond (electronic structure) and (iii) roughening of the surface. The ORR kinetics are much more complex than generally assumed, and even on Pt electrocatalyst, an indirect mechanism for oxygen reduction is possible (Chen and Kucernak 2004). Moreover, oxygen reduction reaction includes the breakage of the O−O bond as well as the formation of the O−H bond. As per literature platinum is the most commonly used electrocatalyst for ORR of all the pure metal ORR catalysts which have been studied to date (Norskov et al., 2004; Peng and Yang 2009).
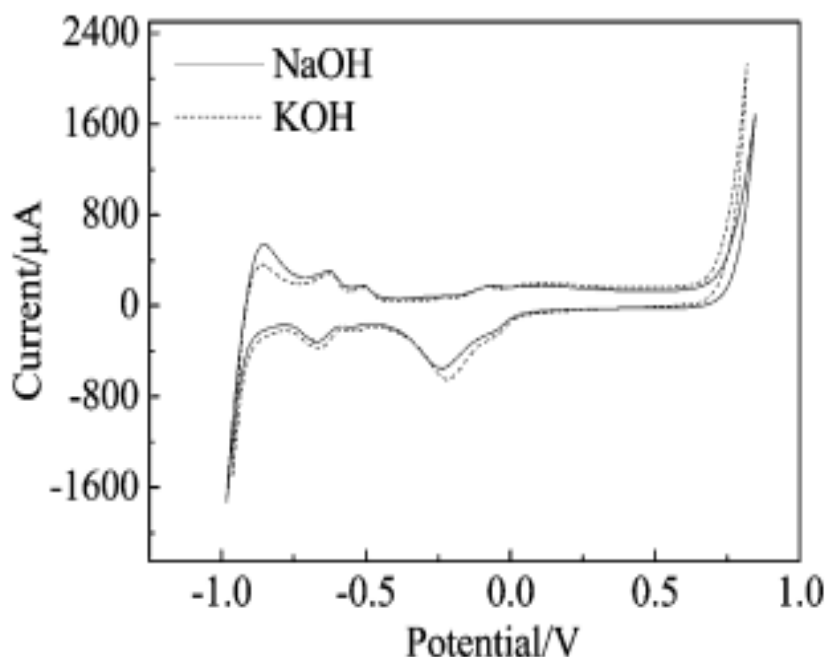
Figure 2.3 CV curves in oxygen-saturated 2 M NaOH and KOH solutions at 298 K, respectively. Scan rate: 100 mV/s (Jin et al., 2010).

Jin et al., (2010) worked on ORR using a polycrystalline Pt surface by cyclic voltammetry techniques, and examined the influence of reaction media on the ORR by comparing the ORR in NaOH and KOH solutions at 25 ^{o}C (Figure 2.3). They observed that a quasi-reversible diffusion controlled reaction, which is mainly dependent on the electrolyte conditions. The KOH solutions were superior to NaOH solutions for the ORR process in both thermodynamic and kinetic consideration. Thus, KOH was used as alkaline medium instead of NaOH in the present study.

It should be noted that considerable efforts have been made over the past decades to develop Pt-alloyed electrocatalysts to boost their catalytic efficiency and stability with reduced content of Pt. The alloyed form of Pt with noble metals (e.g., Au, Pd, Ru, Ag, Rh) or transition metals e.g., Cu, Fe, Co and Ni can also use for ORR (Vliet et al., 2011; Bing et al., 2010; Morozan et al., 2011; Wang et al., 2012). However, they are not so much active for oxygen reduction in fuel cell.

2.1.4.1.5 Physical characterization of anode electrocatalysts

The characterization of synthesised electrocatalyst is very important to known the physical properties. The physical characterizations of synthesized electrocatalyst were mainly performed using X-ray diffraction (XRD), scanning electron microscopy (SEM), energy dispersive X-ray (EDX) and transmission electron microscopy (TEM), which are discussed in below systematically.

2.1.4.1.5.1 X-ray diffraction

The X-ray diffraction (XRD) analysis is performed to find the crystalline structure of acetylene black carbon supported electrocatalyst. The diffraction peak at 2θ of around 25° to the plane (002) is observed for carbon support material. The main peaks for pure Pd appears at 2θ values of 40.1° (111), 46.7° (200) and 68.1° (220) comply with the standard of JCPDS (05 0681). The main peaks as per JCPDS 040802 for pure Pt appear at 2θ values of 39.76^o (111), 46.27^o (200) and 67.5° (220) (Basu et al., 2012). The main peaks for Nickel particle as per JCPDS 04-0850 occurs at 2θ values of 44.56º, 51.76º, and 76.38º corresponding the plane (111), (200) and (220) respectively and the lattice parameter is 0.3523 nm (Houache et al., 2019). The diffraction patterns display the characteristics of crystalline face centered cubic (FCC) of Pd, Pt and Ni, with peaks corresponding to (111), (200), and (220) planes. Nishanth et al., (2011) studied on Pt-Pd alloy electrocatalyst and found that the diffraction peaks for Pt in Pt-Pd alloy catalyst shifted to the higher 2θ values. The shift in the diffraction peaks occurs due to the incorporation of Pd in the FCC structure of Pt, which confirms the alloy formation between Pt and Pd. The lattice parameter of the Pt–Pd alloy was observed between those of pure FCC Pt i.e., 0.3923 nm and pure FCC Pd i.e., 0.3890 nm (Lopes et al., 2008). It also specifies the contraction of the lattice is due to the particle substitution of Pt by Pd in the FCC structure in the formation of the Pt-Pd alloy (Maghsodi et al., 2011).

2.1.4.1.5.2 Scanning electron microscopy

The morphology of synthesized electrocatalyst is characterized by SEM images. It helps to understand the distribution of electrocatalyst particle on support material. The uniform distribution or agglomerated form of electrocatalyst can be easily analysed by the SEM images. However, it is hard to get the size of metal electrocatalysts and carbon from SEM images due to nano size of carbon powder support and loss of clarity in images at higher magnification (Basu et al., 2012). Maghsodi et al., (2011) observed that the SEM images of Pt and Pt-Pd alloyed nanoparticles were agglomerated. Thus, due to agglomeration, the obtained size is larger than crystalline size that has obtained from XRD data.

2.1.4.1.5.3 Energy dispersive X-ray

The surface composition of electrocatalysts are analysed by energy dispersive X-ray (EDX) analysis. It provides the information of elemental surface composition present in the synthesized electrocatalyst in terms of atomic and weight fraction. The EDX composition shows metals and carbon support material as well as oxygen peak due to adsorption of atmospheric oxygen by carbon (Basu et al., 2012). The synthesized electrocatalysts with the desired elements with little differences from the nominal composition is observed, moreover the common impurities if present are also observed in the electrocatalysts using the EDX analysis (Tayal et al., 2012).

2.1.4.1.5.4 Transmission electron microscopy

The particle size and its distribution are obtained by transmission electron microscopy (TEM) analysis. It provides the average particle and detailed morphological observations of electrocatalyst (Basu et al., 2012). The TEM images give the clear view of uniform distribution or agglomerations of particles. The electrocatalyst used in fuel cell are in nano range. Nishanth et al., (2011) observed the particle size of the Pt-Pd particles on

carbon in between 3 and 5 nm. Choudhary et al., (2019) synthesized Pt-Ru/C electrocatalyst and observed almost nano range spherical shape particle with highly disperse and negligible agglomerations on the carbon support material.

2.1.4.2 Cathode oxidant

The most common oxidant used in a fuel cell is oxygen. However, in microfluidic fuel cell liquid based oxidant is used in the form of dissolved solution i.e. dissolved oxygen (Choban et al., 2005; Li et al., 2007; Dector et al., 2013a; Martins et al., 2018a), hydrogen peroxide (Kjeang et al., 2007; Dector et al., 2013b), vanadium ion (Ferrigno et al., 2002; Lee et al., 2012), potassium permanganate (Jindal et al., 2017, Liu et al., 2019), air (Jayashree et al., 2005; Shaegh et al., 2012; Pramanik and Rathoure 2017) and sodium hypochlorite (Kjeang et a., 2008; Martins et al., 2018b).

As discussed above in the cathode electrocatalyst section that the cathodic half cell electro kinetics is sluggish for oxygen reduction reaction on platinum electrocatalyst. The ORR occurs in several individual steps and so most of the of activation overvoltage loss takings place at the cathode side. The slow reactions kinetics in the cathode are combined with low oxygen concentration resulting in low power density when the oxidant in the form of dissolved oxygen is used. As per reported literature, the output power density is very less using dissolved oxygen (0.17 mW/cm^2) compared to KMnO$_4$ (2.4 mW/cm^2) oxidant in microfluidic fuel cell (Choban et al., 2005). Alternate oxidants other than dissolved oxygen can be used to enhance mass transport limitation in electrolyte. The concentration of oxygen in air is four times higher than in aqueous media (Jayashree et al., 2005). The atmospheric oxygen as oxidant can be used to improve the cell performance by changing the design of simple cathode to air breathing cathode.

2.1.4.3 Electrolytes

The electrolyte plays an important role for better performance of a microfluidic fuel cell device. The main purpose of using electrolyte in both the streams i.e., fuel and oxidant is to enhance the ionic conduction and to reduce the ohmic losses in between the anode and the cathode streams. The fuel and oxidant are mixed with electrolyte and then usually fed into the channel using peristaltic and syringe pumps. In microfluidic fuel cells, generally three modes of electrolyte are used (i) acidic (ii) alkaline and (iii) mixed media. The pH of the electrolyte is significantly affecting the reaction kinetics at the individual electrodes, and also the electrode potential at which the electrooxidation or reduction reaction occurs (Choban et al., 2005). The electrolyte used in microfluidic fuel cells is typically a strong acid for acidic medium such as sulphuric acid or a strong base for alkaline medium such as potassium hydroxide which comprises highly mobility of hydronium or hydroxide ions, respectively (Kjeang et al., 2008). Many studies on the electrooxidation of glycerol in alkaline medium using KOH as electrolyte have been reported with improved MFC performance (Dector et al., 2013a; Maya-Cornejo et al,. 2015; Martins et al., 2018a). Thus, in the present work alkaline electrolyte (KOH) was considered.

2.1.5 Cell performance

The literature on glycerol based microfluidic fuel cell suggests that it is still developing as an innovative technology towards the generation of low cost electricity source for low power consuming devices such as portable electronic appliances, pacemaker, glucose sensor mobile phone, laptop computer, health care diagnostics and DNA analysis etc. (Pramanik and Rathoure 2017). Till date many researchers have worked on microfluidic fuel using various types of fuels like methanol (Martins et al., 2018a), ethanol (Armenta-Gonzalez et al., 2016), formic acid (Moreno-zuria et al., 2014), glucose (Galindo et al.,

2012) and ethylene glycol (Lopez-coronel et al., 2019). The oxidant used was air or in some cases H_2O_2 mixed with air (Rathoure and Pramanik 2016) and sodium hypochlorite (Martins et al., 2018b). However, a scanty literature is available on the microfluidic fuel cell using glycerol as fuel in alkaline medium. The main purpose of the research was to improve the cell output i.e., power density from the glycerol based MFC either by design modification of MFC or by the replacement of anode electrocatalysts.

As already discussed, cell architecture and design are very important for fluid delivery within the microchannel and easy assembling of the cell components. It is seen from the literature that the cell performance enhanced significantly, only due to the change in design of the MFCs with similar process conditions like type of electrocatalysts, electrocatalyst loading, cell temperature, glycerol concentration and electrolyte concentration. Similarly, for the MFCs with same design when operated with various types of anode electrocatalysts, the performance got enhanced dramatically only for the change in anode electrocatalysts. However, the reported current density and cell voltage were low. Thus, there is a need for comprehensive studies on various types of MFC design and development of suitable electrocatalysts for glycerol electrooxidation at room temperature.

Dector et al., (2013a) used Y-shaped microfluidic fuel cell with flow over electrode fluid delivery system. The length of the MFC channel was 45 mm and 1 mm depth with an active electrode area of 0.45 cm^2. The synthesized Pd/C and Pd/MWCNT as anode electrocatalyst and commercial Pt/C as cathode electrocatalyst was used for electrooxidation of glycerol. The electrocatalyst ink was deposited on the wall of the channel by spray technique. Very low power densities of 0.70 mW/cm^{2}and 0.51 mW/cm^2 were obtained using Pd/MWCNT and Pd/C electrocatalysts, respectively. Maya-Cornejo et al., (2015) used CuPd/C as anode electrocatalyst for electrooxidation of several fuels

such as methanol, ethanol, glycerol and ethylene glycol in an air breathing nano fluidic fuel cell. The anodic and cathodic electrocatalyst were prepared by spray technique using 2.2 mg of CuPd/C and 2.9 mg Pt/C. The cell performance was obtained in flow through electrode in a high surface area carbon nanoform substrate. The cathode performance was also enhanced using dissolved oxygen and atmospheric oxygen. The maximum power density using glycerol as fuel was 20.43 mW/cm^2. In another work, Maya-Cornejo et al., (2016) synthesized CuPt/C and CuPd/C anode electrocatalyst for electrooxidation of crude and analytical glycerol in air breathing nanofluidic fuel cell. The electrocatalyst CuPd/C and Pt/C of 1 mg was impregnated in carbon nanofoam (Marketech International, Inc) as substrate for each anode and cathode, respectively. The dimension of the electrode in the cell was 20 mm long, 3 mm width and 0.1 mm height with active area of 0.02 cm^2. The maximum power density using CuPd/C were 17.6 mW/cm^2 and 17.4 mW/cm^2 for crude and analytical glycerol, respectively. Similarly, CuPt/C produced maximum power density of 21.8 mW/cm^2 and 23 mW/cm^2 for crude and analytical glycerol at 25 ^{o}C, respectively. The power density were higher for CuPt/C that of CuPd/C. Martins et al., (2018a) studied on mixed media with flow through porous electrode in MFC using glycerol, ethylene glycol and methanol as fuel. Pt/C electrocatalyst was used for both anode and cathode. The KOH of 1 M was used as anode electrolyte and H$_2$SO$_4$ of 1 M as cathode electrolyte. The maximum power density of 39.5 mW/cm^2, 30.3 mW/cm^2 and 30 mW/cm^2 were obtained for the glycerol of 0.05 M, ethylene glycol of 1.5 M of and methanol of 3 M, respectively. Similarly, in another study Martins et al., (2018b) used bleach (sodium hypochlorite) as oxidant which increased the cell performance. The maximum power density of 71.2 mW/cm^2 was obtained in alkaline medium and 315 mW/cm^2 was observed in mixed media configuration with KOH mixed with glycerol and H$_2$SO$_4$ mixed with bleach. Table 2.2 shows the different studies on glycerol based

microfluidic fuel cell by several investigators. All studies are performed using dissolved oxygen or other oxidant like H_2O_2, $KMnO_4$, sodium hypochlorite etc. It is seen from the reported work that the cell performance enhanced by using flow through porous electrode. It is also known as three dimensional flows where contact area between fuel and active sites of electrocatalyst enhances. It is also noted that the anode electrocatalyst were Pd and Pt based for glycerol electrooxidation. However, Pd based electrocatalyst should be investigated more for the study of glycerol electrooxidation in microfluidic fuel cell as Pt is noble metal and not available easily and very expansive. Although many studies have been reported in literature, there are several challenges of microfluidic fuel cells observed like electrode design and fabrication, specially air breathing cathode for better delivery of oxygen from air to the active electrocatalyst sites. Similarly, highly porous anode fabrication is also important. Furthermore, due to its smaller size, microfluidic fuel cells have some concerns. The cross section aspect ratio and electrode configuration significantly affects the cell performance. Thus, it is clear from the detailed literature survey on glycerol based microfluidic fuel cell, it is clear that a thorough experimental study on air breathing microfluidic fuel cell is required to enhance the fuel cell performance in terms of maximum power density by optimizing cell parameters such as type of anode electrocatalyst, electrocatalyst loading, fuel concentration, electrolyte concentration and temperature. It should be noted that, the range of operating parameters must be kept low as possible.

Table 2.2 Performance comparison of different electrocatalyst for glycerol fuel in microfluidic fuel cell.

Fuel and electrolyte used	Oxidant	Device Type/ electrode details/cell temperature	Maximum power density (mW/cm^2)	References
0.1 M glycerol, 0.3 M KOH	Sat. dissolved oxygen	MFC; Anode: Pd/MWCNT $(1.6mg/cm^2)$ Cathode: Pt/C $(0.54\ mg/cm^2)$ Electrode area: $0.45\ cm^2$; Room temperature	0.70	Dector et al., (2013a)
		MFC; Anode: Pd/C $(1.3\ mg/cm^2)$ Cathode: Pt/C $(0.54\ mg/cm^2)$ Electrode area: $0.45\ cm^2$; Room temperature	0.51	
0.1 M glycerol, 0.3 M KOH	Air + sat. dis. oxygen	AB-MNFC; Anode: Cu@Pt /C;2.2 mg/cm^2 Cathode: Pt/C ;2.9 mg $/cm^2$ Electrode area: $0.02\ cm^2$; Temperature: 25 ^{o}C	20.43	Maya-Cornejo et al., (2015)
Glycerol 5 vol%, 0.3 M KOH	Air + sat. dis. oxygen	AB-MNFC; Anode: Cu@Pd/C;1 mg/cm^2 Cathode: Pt/C ;1 mg $/cm^2$ Electrode area: $0.02\ cm^2$; Temperature: 25 ^{o}C	17.41	Maya-Cornejo et al., (2016)
		AB-MNFC; Anode: Cu@Pt/C;1 mg/cm^2 Cathode: Pt/C ;1 mg $/cm^2$ Electrode area: $0.02\ cm^2$; Temperature: 25 ^{o}C	23.16	
0.05 M glycerol, 1 M KOH	KOH, H_2SO_4 (mixed media), sat. dis oxygen	MFC; Anode: Pt/C : 70 mg Cathode: Pt/C: 70 mg Electrode area 0.015 cm^2 Room temperature	39.5	Martins et al., (2018a)
1 M glycerol, 1 M KOH	KOH, H_2SO_4 (mixed media), Sodium hypochlorite	MFC; Anode: Pt/C : 70 mg Cathode: Pt/C: 70 mg Electrode area 0.015 cm^2 Room temperature	315	Martins et al., (2018b)

Abbreviations: MFC, microfluidic fuel cell; AB-MNFC, air breathing membraneless nanofluidic fuel cell; dis., dissolved; sat., saturated.

2.2 Objectives

The detailed literature review reveals that development work on air breathing microfluidic fuel cell in alkaline media based on glycerol fuel is essential as half cell analysis and single cell study show promising results in term of cell voltage and power density. In this context, a detailed study is required to completely understand the various phenomena take place in anode, cathode, and electrolyte of the microfluidic fuel cell. Towards the fulfilling of these requirements, the thesis has following objectives.

1. Design and fabrication of Y-shaped and T-shaped air breathing microfluidic fuel cell setup.

2. Synthesis of palladium based anode electrocatalysts been reported for glycerol electrooxidation and its physical characterization using XRD, SEM, EDX and TEM, and electrochemical characterization in half cell using cyclic voltammetry (CV) and EIS.

3. To study the microfluidic fuel cell for achieving highest power density at the optimum conditions of different operating parameters such as type of electrocatalyst, electrocatalyst loading, glycerol concentration, electrolyte concentration, type of oxidant, flow rate of anode and cathode streams.

4. Optimization of process parameters using response surface methodology (RSM).

5. Stability test of air breathing microfluidic fuel cell.

The next chapter describes the experimental details related to the development of air breathing microfluidic fuel cell in alkaline medium e.g., fabrication of air breathing microfluidic fuel cell setup, anode electrocatalyst preparation, anode and cathode electrode preparation and characterization using half cell analysis through cyclic voltammetry and electrochemical impedance spectroscopy, single cell performance, optimization of process parameters using response surface methodology and stability test of the single cell.